A QM/MM Direct Dynamics Trajectory Investigation of Trimethylene Decomposition in an Argon Bath

Kim Bolton[†] and William L. Hase*

Department of Chemistry, Wayne State University, Detroit, Michigan 48202

Charles Doubleday, Jr.*

Department of Chemistry, Columbia University, New York, New York 10027

Received: July 13, 1998; In Final Form: February 22, 1999

The decomposition of trimethylene embedded in an argon environment is studied using classical trajectory simulations. The trimethylene intramolecular forces are calculated directly from semiempirical electronic structure theory at each trajectory step, and the intermolecular forces are determined from Lennard-Jones 12-6 potential energy functions. When the argon is in a low to moderate density fluid phase, it does not affect the rate of trimethylene decomposition or product branching ratios, but at high densities, the H-transfer reaction leading to propene is favored over cyclization.

Introduction

The intramolecular and unimolecular dynamics of trimethylene and its role in the isomerization of isotopically substituted cyclopropanes have been the subject of extensive experimental[1−10] and theoretical[11−28] investigation. Recently, classical trajectory simulations based on two different potential energy surfaces (PESs) have provided insight into the microscopic details of these reactions.[24−28] One set of studies[24−27] employed the direct dynamics technique,[29] where the energy and forces are obtained directly from electronic structure theory calculations at each trajectory step. These studies were based on a semiempirical PES, with AM1 parameters modified to reproduce CASSCF stationary point properties and experimental activation energies.[24] The resulting PES was called AM1-SRP (AM1 with specific reaction parameters[30,31]). The other study employed an analytic PES where three "critical" degrees of freedom, the central trimethylene CCC angle and the two terminal methylene torsions, were described by functions fit to CASPT2N/6-31G*//GVB-PP(1)/6-31G* energies, and the remaining degrees of freedom were described by molecular mechanics functions.[28]

Simulations of the thermal isomerization of cyclopropane-*1,2-d*$_2$ based on these PESs yielded similar ratios of the rate constants for double methylene rotation, k_{12}, to single methylene rotation, k_1 ($k_{12}/k_1 = 2.3$-3.5 on the AM1-SRP PES[26,27] and 4.7 on the analytic PES[28]). These studies also gave clear evidence that the dynamics of trimethylene is nonstatistical at 695 K.[24−28] The simulated k_{12}/k_1 ratios lie between the experimentally deduced value of 1.0 obtained by Baldwin and collaborators[6] and 5-42 obtained by Berson et al.[3,4] The similarity of the k_{12}/k_1 values obtained from the two PESs and their approximate agreement with experiment supports the use of these PESs to gain insight into trimethylene dynamics at 695 K.

Additional studies, based on the AM1-SRP PES, examined trimethylene decomposition at fixed energies.[24,25] For energies less than 77 kcal mol^{-1} (including zero point energy), the trimethylene dynamics is nonstatistical, in agreement with the data obtained under thermal conditions. At higher energies—between 107 and 146.4 kcal mol^{-1}—the dynamics is statistical and the decomposition single exponential, in agreement with the molecular beam data of Zewail and co-workers.[10] At 146.4 kcal mol^{-1} the simulated unimolecular rate constant of 11 ps^{-1} is similar to the 8.3 ± 1.4 ps^{-1} measured experimentally. This indicates that the AM1-SRP PES also yields valid trimethylene dynamics and decomposition at elevated as well as thermal energies.

In the above simulations the dynamics and decomposition of *isolated* trimethylene molecules were studied, thereby assuming that collisional effects in the molecular beam and thermal experiments are insignificant. Due to the short trimethylene lifetime (tenths of picoseconds[10,24,27]), this is expected to be a good assumption.[32] However, most organic reactions that are performed in the gas, liquid, and matrix environments are expected to be sensitive to collisional and frictional[33,34] effects. An example is the trans → cis isomerization of stilbene, where increasing the collision frequency (buffer gas pressure) leads to an initial increase in the isomerization rate, followed by a decrease at higher collision frequencies (solvent densities).[34,35]

In the present study, collisional and frictional effects on the intra- and unimolecular dynamics of trimethylene are examined. This molecule was chosen since previous studies have provided a detailed microscopic understanding of the unimolecular dynamics of isolated trimethylene, i.e., in a collision free environment. A mixed QM/MM approach[36−39] is used to simulate the decomposition of trimethylene embedded in an Ar environment. Trimethylene intramolecular forces are obtained directly from the AM1-SRP PES, and intermolecular forces are obtained from pairwise Lennard Jones (LJ) 12-6 energy functions. The sensitivity of trimethylene decomposition to collisional and frictional effects is examined over a range of Ar temperatures and densities.

QM/MM Potential Energy Surface

The QM/MM Hamiltonian has the form

[†] Present address: Göteborg University, Department of Chemistry, Physical Chemistry, S-412 96, Göteborg, Sweden.

10.1021/jp982988d CCC: $18.00
Published on Web 04/16/1999

$$H = H_{QM} + H_{MM} + H_{QM/MM} \quad (1)$$

where H_{QM} is the quantum mechanical Hamiltonian, H_{MM} is the molecular mechanics Hamiltonian (which could, in general, include any type of analytic potential energy function), and $H_{QM/MM}$ describes the coupling between the QM and MM subregions. In the laboratory fixed frame the kinetic energy $T(p)$ is a function of the atomic momenta only,[40] and eq 1 can be expressed as

$$H(q, p) = V_{QM}(q) + V_{MM}(q) + V_{QM/MM}(q) + T(p) \quad (2)$$

For the Ar−trimethylene system, $V_{QM}(q)$ is the AM1-SRP PES describing the trimethylene intramolecular energy, $V_{MM}(q)$ is the Ar−Ar intermolecular potential, and $V_{QM/MM}(q)$ describes the Ar−trimethylene interactions.

Trimethylene Intramolecular PES. Features of the AM1-SRP PES, such as stationary point structures, energies, and harmonic vibrational frequencies, have been detailed elsewhere.[24] Using the half-electron method[41] available in MOPAC 7.0,[42] configuration interaction was included in the AM1[43] wavefunction and the resulting PES was fine-tuned to reproduce CASSCF ab initio stationary point features[23] and experimental activation energies.[1,2,5] This was done by scaling the two-center one-electron (resonance) integrals associated with the terminal C−C interactions (to fit cyclization transition state properties) and those associated with C−H interactions between the central hydrogens and the terminal carbons (to fit features of the H-transfer barrier). Inverted Morse-type potential energy terms were appended to the AM1 Hamiltonian to obtain the correct cyclopropane and propene exothermicities. The resulting surface, which bears a close resemblance to the ab initio surface, is illustrated in Figure 1. The curves that link the saddle point structures merely serve to show the connectivity.

The disrotatory saddle point, which has two imaginary frequencies and is 2.2 kcal mol^{-1} above the conrotatory saddle point, and the saddle point for single terminal isomerization, which is 1.4 kcal mol^{-1} above the conrotatory saddle point, are not shown in Figure 1. The disrotatory saddle point structure is C_s and has a CCC angle of 109.6°. At the saddle point for single terminal rotation, the methylene terminals are staggered by 90° and the CCC angle is 111.9°. Whereas this saddle point connects the cis and trans isomers of the (deuterated) cyclopropane on the ab initio surface,[23] it connects the two enantiomeric structures of trimethylene on the AM1-SRP PES.

Two stationary points particularly important for the trimethylene dynamics reported here are the trimethylene minimum and the H-atom transfer transition state. The AM1-SRP harmonic vibrational frequencies for these stationary points, listed in ref 24, are in good agreement with ab initio values.[23,44] The transition states for geometric isomerization have frequencies similar to those for trimethylene.

Intermolecular PES. The intermolecular potential between the Ar atoms, $V_{MM}(q)$, and between the Ar and trimethylene, $V_{QM/MM}(q)$, is described by a sum of pairwise LJ 12-6 functions

$$V = 4\epsilon\left[\left(\frac{\sigma}{r}\right)^{12} - \left(\frac{\sigma}{r}\right)^{6}\right] \quad (3)$$

for Ar−Ar, Ar−C, and Ar−H interactions. The parameters are taken from the PES developed by Lim and Gilbert,[45] where collisional energy transfer between inert gases and large hydrocarbons was studied, and are $\epsilon_{Ar-Ar} = 0.23$ kcal mol^{-1}, $\sigma_{Ar-Ar} = 3.47$ Å, $\epsilon_{Ar-C} = 0.10$ kcal mol^{-1}, $\sigma_{Ar-C} = 3.39$ Å, $\epsilon_{Ar-H} = 0.05$ kcal mol^{-1}, and $\sigma_{Ar-H} = 3.23$ Å. The cutoff for the intermolecular interactions is 7.5 Å. Using larger cutoffs did not change the simulation results. For this investigation, highly accurate intermolecular forces are not necessary since qualitative aspects of the Ar environment are investigated. Interactions between atomic partial charges, which partially account for polarization effects and are included in the study of Lim and Gilbert, are not included in this work. By excluding polarization effects, which would also have to be incorporated into the AM1-SRP Hamiltonian,[36] the focus is on collisional and frictional effects only, not on electronic changes of the trimethylene PES due to the presence of the environment. This is referred to as *mechanical* embedding of trimethylene in an Ar bath.[38]

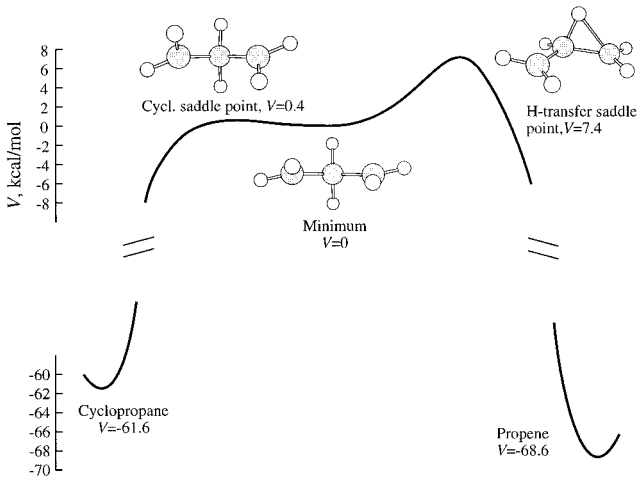

Figure 1. . Minimum potential energy along the cyclopropane ↔ trimethylene ↔ propene reaction path.

Trajectory Methods

Trajectory Initialization. The simulations employed periodic boundary conditions,[46] with the trimethylene initialized at the center of a 20 Å × 20 Å × 20 Å box (or 16 Å × 16 Å × 16 Å at higher densities) and surrounded by a thermalized Ar bath. The trimethylene had an initial energy (including the 47.3 kcal mol^{-1} zero point energy) of 54.6 or 146.4 kcal mol^{-1} and was rotationally cold. Under collision free conditions, trimethylene decomposition is nonstatistical at the lower energy and statistical at the higher energy.[23]

The efficient microcanonical[47] and quasiclassical normal mode[48] sampling procedures, which have been detailed elsewhere,[23] were used to select the initial trimethylene Cartesian coordinates and momenta. By using two sampling schemes, the effects of the initial conditions on the ensuing intra- and unimolecular dynamics were ascertained. The efficient microcanonical sampling (EMS) scheme, which takes anharmonic effects in account, prepares microcanonical ensembles of the total trimethylene classical phase space. The dividing surface between trimethylene and cyclopropane was defined in terms of the trimethylene CCC angle. The transition states (TS) are at CCC = 94° for an energy of 54.6 kcal mol^{-1} and CCC = 89° for 146.4 kcal mol^{-1}. EMS sampling over a range of CCC angles showed[23] that these are the classical anharmonic variational[49−51] transition states for these energies. The dividing surface between trimethylene and propene is assumed to be at the H-transfer barrier (see Figure 1) and is thus energy independent.

For quasiclassical normal mode sampling, the initial conditions are selected from a statistical sampling of quasiclassical, harmonic vibrational states at the H-transfer barrier.[23] Each state

with an energy less than the total trajectory energy has an equal probability of being selected. The difference in the total energy and the energy of the selected state is placed in the reaction coordinate, giving it an energy distribution in accord with RRKM theory.[52,53] The initial reaction coordinate momentum is directed toward trimethylene. Random phases are selected for the normal mode coordinates and momenta before the Cartesian coordinates are determined from the standard linear transformation.[54] Since this transformation is not exact at finite energies, the Cartesian coordinates and momenta are scaled to obtain the desired trimethylene energy. This scaling is not severe, with the average difference between the unscaled and scaled energies being ≈10% of the desired energy.

The Ar bath was initialized using a thermal Monte Carlo (MC) sampling procedure.[46] To initiate the sampling, the Ar atoms were placed on a grid surrounding the trimethylene, such that they were uniformly distributed in the periodic box. By fixing the trimethylene coordinates and momenta during the Ar thermalization, the trimethylene energy distribution, chosen by EMS or quasiclassical sampling, was not affected. Although the thermal conditions obtained from the MC sampling do not depend on the initial Ar positions, the number of MC steps required to achieve thermalization is sensitive to their initial location. For moderate Ar densities, $6 \times 10^{-3} \leq \rho \leq 2.5 \times 10^{-2}$ atoms Å^{-3}, thermalization was obtained in 10^5 MC steps (for all temperatures 100 K $\leq T \leq$ 1000 K). Thermal equilibrium conditions were identified by a constant average potential energy.[46] At higher densities, $\rho = 6-7 \times 10^{-2}$ atoms Å^{-3}, about 5 times as many MC steps were required for thermalization. Due to the computational expense (of MC and MD), the box length was decreased from 20 to 16 Å for these high densities. All Ar atoms were moved at each MC step, and the step size was chosen so that ≈50−60% of trial configurations were accepted in the Markov chain. At the lowest density ($\rho = 6.25 \times 10^{-3}$ atoms Å^{-3}) there were 50 Ar atoms in the periodic box, and at the highest density ($\rho = 7.32 \times 10^{-2}$ atoms Å^{-3}) there were 300 atoms.

The initial conditions for the first MD trajectory in each ensemble were obtained after the above MC "meltdown" period. The initial conditions of subsequent trajectories were obtained after 5000 MC steps, where the sampling was started from the initial Ar positions of the previous trajectory. Using these positions, instead of reinitializing the Ar atoms on their grid positions, allowed for thermalization after the smaller number of MC steps, thereby improving the simulation efficiency. A total of 5000 steps were required to eliminate correlation between the initial conditions of successive trajectories and to ensure rethermalization of the Ar bath surrounding new trimethylene geometries (chosen for each trajectory from EMS or quasiclassical sampling).

To summarize, there are two steps in the sampling of initial conditions. First, 54.6 or 146.0 kcal mol^{-1} of vibrational energy is added to trimethylene with EMS or quasiclassical normal mode sampling. Trimethylene is then placed in the center of a box, with periodic boundary conditions, and surrounded by an argon bath with an equilibrium temperature and density. Initially, trimethylene is in a nonequilibrium state with respect to the bath, since its coordinates and momenta are held fixed when the bath is equilibrated.

Trajectory Integration. Cartesian coordinates and momenta were integrated by solving Hamilton's equations with a combined fourth order Runge−Kutta and sixth order Adams−Moulton predictor−corrector integration algorithm[55,56] as implemented in VENUS-MOPAC.[57] At each time step Schrödinger's equation is solved for the trimethylene intramolecular energies and forces using the appropriate MOPAC 7.0[42] subroutines. Once a converged SCF wavefunction has been obtained and configuration interaction included, the trimethylene atomic forces are determined analytically. By starting the SCF convergence using the optimized molecular orbital coefficients from the previous trajectory step, only 6−10 SCF iterations are required at each step. The intermolecular forces are the first derivatives of the LJ 12-6 energy functions with respect to the Cartesian coordinates and are added to the trimethylene intramolecular forces to give the total forces.

The velocity scaling procedure of Berendsen et al.[58] was used to maintain a constant Ar temperature. At each time step the Ar velocities are scaled by

$$\lambda = \left[1 + \frac{\Delta t}{\tau}\left(\frac{T}{T_{\text{ins}}} - 1\right)\right]^{1/2} \tag{4}$$

where Δt is the trajectory time step, τ is a smoothing factor, T is the desired temperature and T_{ins} is the instantaneous temperature

$$T_{\text{ins}} = \frac{2}{(3N-3)k_b}\sum_{i=1}^{N}\frac{1}{2}m v_i^2 \tag{5}$$

where N is the number of Ar atoms, k_b is the Boltzmann factor, m is the Ar mass, and v_i are the atomic velocities. If $\tau = \Delta t$, the Ar temperature is set exactly to T at each time step, which may induce artificial noise or chaos into the simulation. For τ greater than Δt, the Ar temperature approaches, but does not equal, T and the stochastic perturbations to the atomic velocities are not as severe. A larger value of τ also allows for local heating of the Ar bath in the vicinity of the trimethylene. Different temperature scaling rates were investigated by varying τ around 10 fs, and since the simulation results were insensitive to these variations, a τ of 10 fs ($\Delta t = 0.25$ fs) was used for the simulations reported here. The insensitivity to variations in τ indicates that similar simulation results would be obtained with other algorithms, e.g., the Nosé−Hoover thermostat,[59] for maintaining the temperature of the Ar bath.

Trajectories were integrated with a step size of 0.25 fs, which in the absence of temperature scaling ($\tau \rightarrow \infty$), conserved the energy to four significant figures over the length of each trajectory. The trajectories were propagated until either cyclopropane or propene was formed. The criterion for cyclopropane formation was that the central CCC angle decreased to 75°. This is 19° smaller than at the variational cyclization transition state for a trimethylene energy of 54.6 kcal mol^{-1} and 14° smaller than that at 146.4 kcal mol^{-1} and facilitated the monitoring of TS recrossings. The criterion for propene formation was that a central CH bond was at least 2.3 Å with the H-atom being closer than 1.3 Å to a terminal carbon. Since these configurations lie on the propene side of the H-transfer barrier, this criterion also allows for evaluation of TS recrossings.

Analysis of Trajectory Data. Collisional energy transfer was studied by monitoring trimethylene intramolecular and rotational energies over time. In particular, collisional energy transfer can be observed as a broadening of the trimethylene energy distributions, where each distribution is obtained from energies monitored over the trimethylene lifetime. Distributions were obtained by calculating energies every tenth trajectory step (i.e., every 2.5 fs) for all 150 trajectories in the ensemble and binning these data to yield histograms. The resulting distributions are averages over the lifetimes of the trimethylene molecules.

In accordance with the no recrossing assumption of RRKM theory,[52,53] cyclopropane:propene branching ratios, N_{cyc}:N_{prop}, were obtained from the first crossing of the cyclization or H-transfer barrier, i.e., N_{cyc} is the number of trajectories crossing the cyclization barrier and N_{prop} the number crossing the H-transfer barrier. Effects of recrossings were determined by comparing N_{cyc}:N_{prop} with the ratio of the number of trajectories forming cyclopropane and propene products. The branching ratios are normalized, i.e.,

$$\mathrm{BR} = \left(\frac{N_{cyc}}{N_{cyc} + N_{prop}}\right):\left(\frac{N_{prop}}{N_{cyc} + N_{prop}}\right) \tag{6}$$

Decay rate constants were also obtained from the first time that trajectories crossed the cyclization or H-transfer barrier. In accordance with RRKM theory,[52,53] they are determined by fitting the simulated lifetime distribution, $P(t)$, with a single exponential function

$$P(t) = -\frac{1}{N(0)}\frac{\mathrm{d}N(t)}{\mathrm{d}t} = k_e^{-kt} \tag{7}$$

where $N(t)$ is the number of trajectories that have not reacted at time t and k is the rate constant. If the decay is biexponential, it is fit with the sum of two exponentials, i.e.,

$$S(t) = \frac{N(t)}{N(0)} = A\mathrm{e}^{-k_1 t} + B\mathrm{e}^{-k_2 t} \tag{8}$$

where A and B are the fraction of trajectories decomposing with rate constants k_1 and k_2, respectively. Effects of barrier recrossings are evaluated using eqs 7 and 8, but with t being the final time of barrier crossing before product formation, and comparing rate constants determined in this manner with those obtained from the first time of barrier crossing.

Three properties that provide structural and dynamic information of the Ar environment are the reduced density, ρ^*, the diffusion constant, D, and the radial distribution function, $g(r)$.[46,60] The reduced density is

$$\rho^* = \frac{N\sigma^3}{V} = \rho\sigma^3 \tag{9}$$

where N is the number of Ar atoms, V is the volume of the periodic box, and σ^3 is the excluded volume of an Ar atom, calculated from the LJ σ. The presence of the trimethylene, which slightly reduces the volume V, is ignored.

The diffusion rate constant is[46]

$$\mathrm{D} = \frac{\mathrm{MSD}}{6t} \tag{10}$$

where the mean square displacement (MSD) over time $t = t_f - t_i$ is

$$\mathrm{MSD} = \frac{<\sum_{j=1}^{N}(r_j(t_f) - r_j(t_i))^2>}{N} \tag{11}$$

The sum in eq 11 is over all Ar atoms and $r_j(t_i)$ and $r_j(t_f)$ are the positions of atom j at the initial and final times t_i and t_f, respectively. The averaging is over all time origins, t_i, along the trajectory with $t = t_f - t_i$ held fixed. Since relatively long trajectories are required to obtain the diffusion constants and calculating AM1-SRP forces is computationally demanding, these simulations were done in the absence of trimethylene. The presence of trimethylene is not expected to significantly affect the diffusion rates since the radial distribution function, which measures the structure of the Ar environment, is the same in the presence or absence of trimethylene. To determine the diffusion rate constant, a 100 ps trajectory was propagated with a step size of 1 fs.

TABLE 1: Cyclopropane:Propene Branching Ratios for $\rho^* = 0.52$

	$E = 54.6$ kcal mol^{-1}		$E = 146.4$ kcal mol^{-1}	
T/K	EMS[a]	barrier[b]	EMS	barrier
100	0.86:0.14	0.77:0.23	0.45:0.55	0.43:0.57
200	0.82:0.18	0.83:0.17	0.47:0.53	0.47:0.53
300	0.88:0.12	0.81:0.19	0.50:0.50	0.47:0.53
500	0.83:0.17	0.88:0.12	0.52:0.48	0.40:0.60
800	0.83:0.17	0.81:0.19	0.57:0.43	0.47:0.53
1000	0.85:0.15	0.79:0.21	0.54:0.46	0.44:0.56

[a] Trajectories were initialized with EMS. sampling. [b] Trajectories were initialized with normal mode sampling at the H-transfer barrier.

The radial distribution function is[46]

$$g(r) = \frac{V}{N^2}<\sum_i \sum_{j\neq i}\delta(r - r_{ij})> \tag{12}$$

where i and j index the Ar atoms and the average is over all Ar pairs. To implement eq 12, the delta function is replaced by small intervals (or bins) such that, within a certain range of Ar−Ar separations, each interval has a finite number of entries. This yields a histogram comprising all Ar−Ar separations that fall within that range. The radial distributions presented in the next section are representative of complete trajectories (or ensembles of trajectories) and are obtained by averaging over distributions evaluated at every tenth trajectory step.

Results and Discussion

Table 1 shows the cyclopropane:propene branching ratio as a function of initial trimethylene energy, initialization method, and Ar temperature for $\rho^* = 0.52$. This is slightly below the reduced triple point density for LJ fluids, $\rho_t^* = 0.85$.[60] The lowest temperature, 100 K, is between the triple point and critical temperatures for Ar ($T_t = 84$ K and $T_c = 151$ K).[60] The higher temperatures at this reduced density pertain to fluid Ar and the lowest temperature to the gas−liquid two-phase region.[60] The branching ratios do not change significantly over this temperature range and are similar to the branching ratios obtained in a collision free environment.[24] For the isolated molecule at 54.6 kcal mol^{-1}, BR = 0.90:0.10 when using EMS sampling and 0.84:0.16 when sampling at the H-transfer barrier. At 146.4 kcal mol^{-1} they are 0.51:0.49 and 0.49:0.51 for EMS and barrier sampling, respectively. There are no recrossing effects on the branching ratios at the T,ρ^* combinations shown in Table 1.

For the Ar density in Table 1, the thermal decomposition rates are similar to what was found from previous calculations for a collision free environment.[24] When using EMS sampling at 54.6 kcal mol^{-1}, the decay is double exponential. With Ar present, the short lifetime trajectories have a rate constant between 7.5 (100 K) and 11 ps^{-1} (300 K), while the long lifetime trajectories decompose with a rate constant between 3.5 (100 K) and 5 ps^{-1} (300 K). These are similar to the rates constants of 9 and 3 ps^{-1} obtained under collision free conditions.[24] For barrier sampling, the 54.6 kcal mol^{-1} decom-

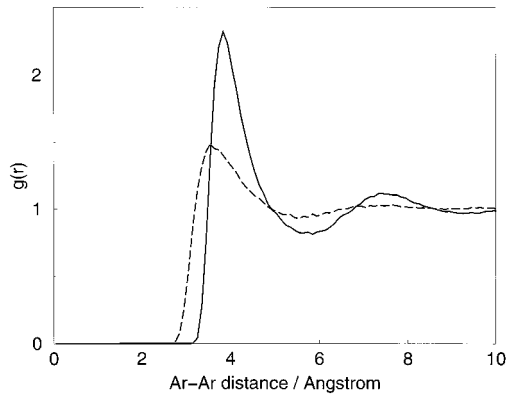

Figure 2. Radial distributions for Ar at 100 K (solid line) and 1000 K (dashed line) for $\rho^* = 0.52$.

position is single exponential with a rate constant between 1.7 (100 K) and 3.0 ps^{-1} (800 K), which is also similar to the single exponential rate constant of 3 ps^{-1} obtained for the isolated molecule. At the higher energy of 146.4 kcal mol^{-1}, the decomposition is a single exponential in both the presence and absence of Ar. This is the case for both sampling methods. With Ar present, the rate constant is between 12 (800 K) and 16 ps^{-1} (300 K) for EMS sampling and between 12.5 (200 K) and 13 ps^{-1} (1000 K) for barrier sampling. These are similar to the rate constants of 14 and 12 ps^{-1} observed for the isolated molecule with EMS and barrier excitation, respectively. The are no effects of barrier recrossing on the rate constants.

The diffusion rate constants for the T,ρ^* combinations shown in Table 1 are on the order of $10^{-3}-10^{-2}$ cm^2 s^{-1} (at 1000 K, $D = 3.0 \times 10^{-2}$ cm^2 s^{-1} and at 100 K it is 2.5×10^{-3} cm^2 s^{-1}). They pertain to Ar dynamics in the fluid region (at temperatures above 151 K[60]) or in the gas−liquid two-phase region (at 100 K[60]) and are thus larger than the diffusion rate constant of liquid Ar,[60] which is $\approx 1.6 \times 10^{-5}$ cm^2 s^{-1}. The radial distributions obtained at 100 and 1000 K are shown in Figure 2. At both temperatures the Ar fluid is structured, with two distinct peaks in the radial distribution at 100 K. In spite of this structure and the relatively fast diffusion rates for the conditions in Table 1, the Ar collisions do not affect the branching ratios or unimolecular decomposition rates. This may be due to the very short trimethylene lifetimes (on the order of tenths of picoseconds) and the small stereochemical size associated with the reaction coordinates (H motion for propene formation and terminal CH_2 rotation/CCC angle bend for cyclization).

The collisional energy transfer is seen by the change in trimethylene intramolecular and rotational energies over time. Intramolecular and (average) rotational energy are conserved for the isolated molecule, but collisions with the Ar bath will lead to a broadening in the distribution of these energies. Figure 3 shows the distributions in intramolecular and rotational energies, sampled over the entire trimethylene lifetime and all trajectories in the ensemble, when EMS was used to initialize trimethylene with an energy of 146.4 kcal mol^{-1} ($J = 0$). The plots are for Ar temperatures of 100 and 1000 K. Similar distributions are obtained for all conditions listed in Table 1. Although there is some broadening in the distributions, the collisional energy transfer is not sufficient to affect the trimethylene branching ratios and decomposition rates.

Table 2 shows the branching ratios for 1000 K when varying the Ar density, initial trimethylene energy, and the initialization method. The four lowest densities, $0.26 \leq \rho^* \leq 1.04$, span the range from low to moderate Ar fluid densities ($\rho_t^* = 0.85$).

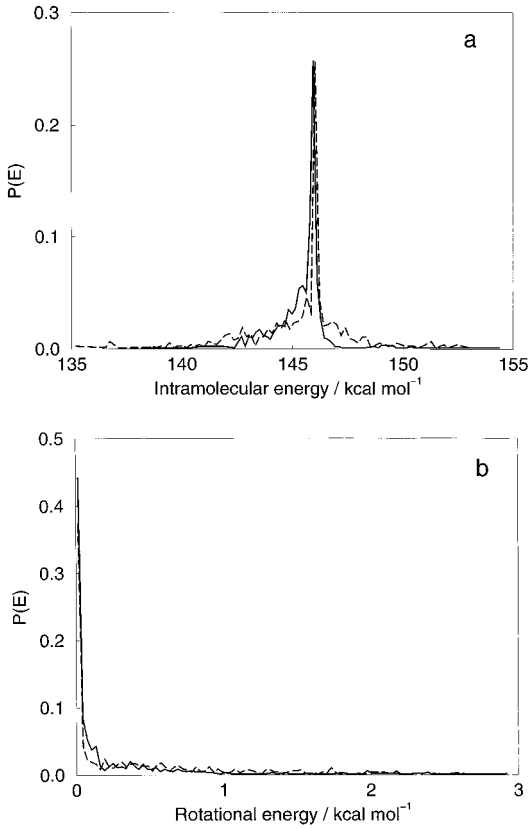

Figure 3. Normalized intramolecular (panel a) and rotational (panel b) energy distributions of trimethylene when EMS was used to initialize trimethylene with an energy of 146.4 kcal mol^{-1} ($J = 0$). The plots are for Ar temperatures of 100 K (solid lines) and 1000 K (dashed lines) and $\rho^* = 0.52$. The energy distributions are averaged over the trimethylene lifetimes.

TABLE 2: Cyclopropane:Propene Branching Ratios at 1000 K

	$E = 54.6$ kcal mol^{-1}		$E = 146.4$ kcal mol^{-1}	
ρ^*	EMS[a]	barrier[b]	EMS	barrier
0.26	0.90:0.10	0.82:0.18	0.56:0.44	0.50:0.50
0.52	0.85:0.15	0.79:0.21	0.54:0.46	0.44:0.56
0.78	0.89:0.11	0.81:0.19	0.46:0.64	0.39:0.61
1.04	0.87:0.13	0.85:0.15	0.56:0.44	0.38:0.62
2.81	0.38:0.62	0.37:0.63	0.55:0.45	0.03:0.97
3.06	0.02:0.98	0.01:0.99	0.01:0.99	0.03:0.97

[a] Trajectories were initialized with EMS sampling. [b] Trajectories were initialized with normal mode sampling at the H-transfer barrier.

Except for barrier sampling at 146.4 kcal mol^{-1}, where there is a small decrease in the branching ratio with increasing density, there are no significant collisional effects at these densities. The branching ratios and decomposition rates are similar to those of the isolated molecule (the range in rates is similar to that when varying the temperature at $\rho^* = 0.52$), and there are no significant recrossing effects.

At the four lowest densities listed in Table 2 the diffusion rate constants range from 6.0×10^{-3} cm^2 s^{-1} ($\rho^* = 1.04$) to 6.5×10^{-2} cm^2 s^{-1} ($\rho^* = 0.26$) and, since these densities pertain to the fluid region at 1000 K, are larger than the diffusion rate of liquid Ar. The radial distribution functions obtained for this density range reveal that the Ar fluid is structured, especially at the higher densities, with two distinct solvation shells (similar to that seen for $\rho^* = 0.52$, $T = 100$ K in Figure 2). The collision-induced broadening in the trimethylene intramolecular and rotational energies is similar to that shown in Figure 3. Even

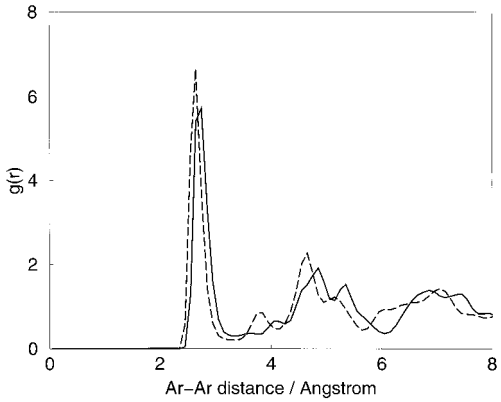

Figure 4. Radial distributions for Ar at $\rho^* = 2.81$ (solid line) and 3.06 (dashed line) and $T = 1000$ K.

though the collisions are sufficient to induce slight changes in the trimethylene energies, they do not affect the branching ratios and decomposition rates.

The two largest densities listed in Table 2, $\rho^* = 2.81$ and 3.06, are far larger than the reduced triple point density for LJ fluids and pertain to a very high density fluid or even a solid/matrix environment. Over a 100 ps trajectory the Ar atoms move, on average, just 1.8 Å at $\rho^* = 2.81$ and 0.9 Å at $\rho^* = 3.06$. This is less than the 2.5 Å diameter of the Ar excluded volume (see the position of the first solvation shell in Figure 4), showing that the Ar atoms have not diffused out of their fluid/matrix cage. Diffusion rate constants are thus not calculated for these densities. The small average displacements of the Ar atoms yield radial distribution functions, shown in Figure 4, that are not as smooth as those obtained at lower densities. The Ar environment is highly structured at these T,ρ^* combinations, and there is a large cagelike[61] frictional effect[34,62] on the branching ratios (see Table 2). The Ar environment favors H-transfer over cyclization, although for $\rho^* = 2.81$ the branching ratios depend on the initial trimethylene energy and trajectory initialization procedure. For an initial trimethylene energy of 54.6 kcal mol^{-1}, the branching ratio is similar for both sampling methods, and there is a fairly strong bias for H-transfer. At 146.4 kcal mol^{-1} the Ar has very little effect on the branching ratio when initializing using EMS, but when exciting at the barrier, almost all trajectories form propene. At $\rho^* = 3.06$, H-transfer is strongly favored over cyclization for both energies and initialization procedures.

The change in the branching ratios at high densities is due to frictional effects and collisional energy transfer. Figure 5 shows the broadening in the intramolecular and rotational energy distributions, obtained from sampling energies over the trimethylene lifetime, for these densities when the initial trimethylene energy is 146.4 kcal mol^{-1} and EMS was used to initialize the trajectories. Similar broadening is seen when exciting trimethylene at the barrier and at a trimethylene energy of 54.6 kcal mol^{-1}. The inset in Figure 5a shows the ensemble-averaged trimethylene intramolecular energy over the trimethylene lifetime. At these high densities the Ar cage that encloses the trimethylene is small, and this leads to a rapid compression of the trimethylene (which is not initially in equilibrium with the Ar bath) and hence to an increase in its intramolecular energy (this increase in energy may be regarded as a cage or collision effect). Subsequent collisions with the bath molecules lead to a cooling of the trimethylene. Since the trimethylene lifetime is ≈50−80 fs under these conditions, the trimethylene decays at high energies (300−400 kcal mol^{-1}). It is difficult to elucidate the relative sensitivity of the branching ratio to the increase in

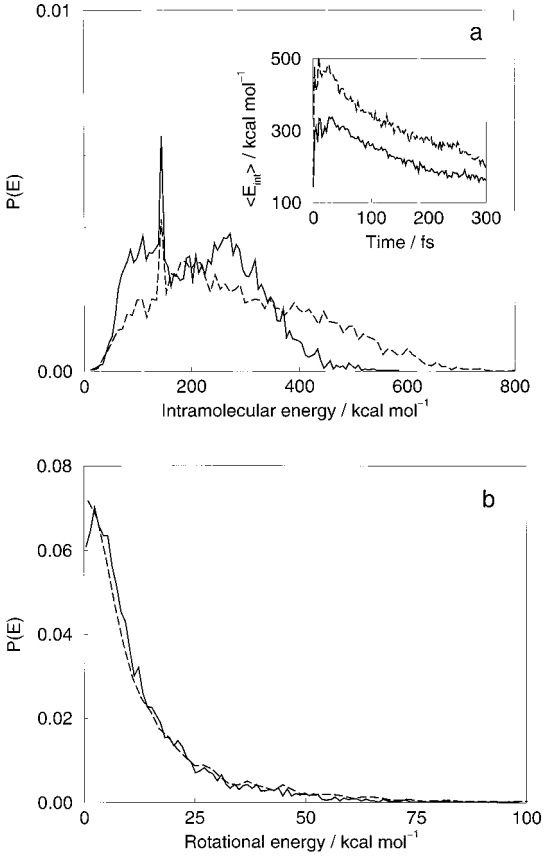

Figure 5. Same as for Figure 3, except the plots are for Ar reduced densities of 2.81 (solid line) and 3.06 (dashed line) and $T = 1000$ K. The inset in panel a shows the time dependence of the ensemble averaged trimethylene intramolecular energy, $\langle E_{int} \rangle$.

trimethylene intramolecular energy and the frictional effects of the Ar cage that may lead to closure of the cyclization channel. The bias toward H-transfer (which involves the motion of a sterically small hydrogen atom) over cyclization (which involves sterically larger CH_2 rotation and CCC angle bending) indicates that these frictional effects may dominate. However, the trimethylene lifetime does not increase at high Ar densities, which is expected if frictional effects hinder cyclization (which is a major reaction channel for the isolated molecule). In some cases the lifetime decreases slightly (up to ≈5% of the isolated molecule lifetime), which is associated with decomposition at higher trimethylene energies.[24] Under collision free conditions, an increase in the trimethylene energy decreases the cyclization: propene branching ratio but does not lead to the closure of the cyclization decomposition channel.[24]

Summary

A mixed QM/MM direct dynamics trajectory technique, based on an AM1-SRP model for the trimethylene PES, has been used to study collisional and frictional effects of an Ar environment on the decomposition of trimethylene. For a reduced Ar density of 0.52, which is slightly below the reduced triple point density of LJ fluids, trimethylene decomposition is not affected by the environment over a 100−1000 K temperature range. Similarly, at 1000 K and for reduced densities between 0.26 and 1.04, the Ar fluid does not affect the rate constants or cyclopropane: propene branching ratios.

At 1000 K and reduced densities of 2.81 and 3.06, the effects of the Ar environment increase the relative number of reactions that lead to propene formation. This is probably a combined

result of frictional effects that retard cyclization more than H-transfer and the large increase in trimethylene intramolecular energy due to its compression by the Ar environment.

Semiempirical electronic structure theoretical methods are attractive for QM and QM/MM classical trajectory simulations in comparison to ab initio methods, such as Hartree−Fock, MP2, and density functional theory, because of the excessive computer time required for the latter.[29] However, considerable care has to be taken in using a semiempirical method to study unimolecular reaction dynamics, since the parameters of the model may only qualitatively represent the reaction's PES. Some of the arbitrariness in the parameterization of the semiempirical model is removed by choosing SRPs,[30,31] as is done here, but this reparameterization may not insure a sufficiently accurate PES.[63] This has been shown for AM1-SRP models of H_2CO and $Cl^- - CH_3Br$ dissociation.[63,64] The accuracy of the AM1-SRP PES should be tested by comparison with both experimental data and high-level ab initio calculations. Such tests indicate that the trimethylene AM1-SRP PES used in this work is a valid model for studying trimethylene's kinetics and dynamics.

Previous comparisons of classical trajectories with experiment and quantum dynamics have shown that trajectories give accurate descriptions of short-time unimolecular and intramolecular dynamics.[65−70] Thus, the trajectory approach used here is expected to be adequate for probing the dynamics of the short-lived trimethylene biradical. In this regard, it is noteworthy that a quantum dynamical simulation[71] of the geometric isomerization of trimethylene gives a product branching ratio nearly identical to that determined from trajectories. For molecules with long lifetimes, the unphysical flow of zero point energy (zpe) may artificially enhance intramolecular vibrational energy redistribution and unimolecular reaction rates.[72−74]

In future work it may be of interest to determine whether zpe flow affects the unimolecular dynamics of the isolated trimethylene biradicals in the gas phase.[75] For this condition, the principle unimolecular reactions for trimethylene are geometric isomerization and ring closure to form cyclopropane. The dynamics of these reactions is expected to be dominated by trimethylene's low-frequency torsional, CCC bending, and CH_2 wagging modes, with the high-frequency CH stretch and bending modes making at most only a minor contribution. Several approaches could be used to determine whether the relatively large zpe values of these modes affect the classical trajectory reaction rates. One would be to simply exclude zpe from these modes in the initial conditions for the trajectories. For another, stiff potential terms could be added to the AM1-PES for these modes to decouple them from the remaining modes of trimethylene.[76] Finally, a more rigorous approach would involve a mixed classical−quantum simulation, where the high-frequency modes of trimethylene are treated quantum dynamically, e.g., by the time-dependent self-consistent field (TDSCF) method,[77] and the lower frequency trimethylene modes are treated classically.

There are several additional properties of the Ar−trimethylene system which could be investigated. In addition, it is important to consider technical aspects of the QM/MM direct dynamics trajectory approach to make the computations more efficient and thus have a broader range of applications. It would be of interest to study trimethylene's kinetics in other rare or unreactive gases to see if there are any general trends in the kinetics versus temperature and density. It would also be of interest to calculate the pair distributions for the distances between the gas and H and C atoms, since they may give some information to how the gas packs around the trimethylene molecule at various densities and temperatures. Furthermore, it may be possible to distinguish between frictional and collisional effects in trimethylenes condensed phase kinetics by simply running constant temperature-constant pressure molecular dynamics with an inert gas present.[78] Finally, it may be possible to enhance the efficiency of the simulations by using a multiple time step integrator,[79,80] with a long time step for the inert gas and a shorter time step for trimethylene. A Verlet[81] or other symplectic integrator[82−84] may be adequate for the inert gas.

Acknowledgment. K.B. and W.L.H. are grateful for financial support from the National Science Foundation (CHE-94-03780). C.D. is grateful for financial support from the same source (CHE-94-20826).

References and Notes

(1) Schlag, E. W.; Rabinovitch, B. S. *J. Am. Chem. Soc.* **1960**, *82*, 5996.
(2) Waage, E. V.; Rabinovitch, B. S. *J. Phys. Chem.* **1972**, *76*, 1965.
(3) Berson, J. A.; Pedersen, L. D. *J. Am. Chem. Soc.* **1975**, *97*, 238.
(4) Berson, J. A.; Pedersen, L. D.; Carpenter, B. K. *J. Am. Chem. Soc.* **1976**, *98*, 122.
(5) Rabinovitch, B. S. *Chem. Phys.* **1982**, *67*, 201.
(6) Cianciosi, S. J.; Ragunathan, N.; Freedman, T. B.; Nafie, L. A.; Lewis, D. K.; Glenar, D. A.; Baldwin, J. E. *J. Am. Chem. Soc.* **1991**, *113*, 1864.
(7) Freedman, T. B.; Cianciosi, S. J.; Ragunathan, N.; Baldwin, J. E.; Nafie, L. A. *J. Am. Chem. Soc.* **1991**, *113*, 8298.
(8) Baldwin, J. E.; Cianciosi, S. J. *J. Am. Chem. Soc.* **1992**, *114*, 9401.
(9) Baldwin, J. E.; Cianciosi, S. J.; Glenar, D. A.; Hoffmann, G. J.; Wu, I-W.; Lewis, D. K. *J. Am. Chem. Soc.* **1992**, *114*, 9408.
(10) Pedersen, S.; Herek, J. L.; Zewail, A. H. *Science* **1994**, *266*, 1359.
(11) Smith, F. T. *J. Chem. Phys.* **1958**, *29*, 235.
(12) Benson, S. W. *J. Chem. Phys.* **1961**, *34*, 521.
(13) Hoffmann, R. *J. Am. Chem. Soc.* **1968**, *90*, 1475.
(14) O'Neal, H. E.; Benson, S. W. *J. Phys. Chem.* **1968**, *72*, 1866.
(15) Horsely, J. A.; Jean, Y.; Moser, C.; Salem, L.; Stevens, R. M.; Wright, J. S. *J. Am. Chem. Soc.* **1972**, *94*, 279.
(16) Hay, P. J.; Hunt, W. J.; Goddard, W. A., III *J. Am. Chem. Soc.* **1972**, *94*, 638.
(17) Kollmar, H. *J. Am. Chem. Soc.* **1973**, *95*, 966.
(18) Jean, Y.; Chapuisat, X. *J. Am. Chem. Soc.* **1974**, *96*, 6911.
(19) Chapuisat, X.; Jean, Y. *J. Am. Chem. Soc.* **1975**, *97*, 6325.
(20) Yamaguchi, Y.; Schaefer, H. F., III; Baldwin, J. E. *Chem. Phys. Lett.* **1991**, *185*, 143.
(21) Getty, S. J.; Davidson, E. R.; Borden, W. T. *J. Am. Chem. Soc.* **1992**, *114*, 2085.
(22) Baldwin, J. E.; Yamaguchi, Y.; Schaefer, H. F., III *J. Phys. Chem.* **1994**, *98*, 7513.
(23) Doubleday, C., Jr. *J. Phys. Chem.* **1996**, *100*, 3520.
(24) Doubleday, C., Jr.; Bolton, K.; Peslherbe, G. H.; Hase, W. L. *J. Am. Chem. Soc.* **1996**, *118*, 9922.
(25) Bolton, K.; Hase, W. L.; Doubleday, C., Jr. *Ber. Bunsenges. Phys. Chem.* **1997**, *101*, 414.
(26) Doubleday, C., Jr.; Bolton, K.; Hase, W. L. *J. Am. Chem. Soc.* **1997**, *119*, 5251.
(27) Doubleday, C., Jr.; Bolton, K.; Hase, W. L. *J. Phys. Chem.* **1998**, *102*, 3648.
(28) Hrovat, D. A.; Fang, S.; Borden, W. T.; Carpenter, B. K. *J. Am. Chem. Soc.* **1997**, *119*, 5253.
(29) Bolton, K.; Hase, W. L.; Peslherbe, G. H. In *Multidimensional Molecular Dynamics Methods*; Thompson, D. L., Ed.; World Scientific: New Jersey, 1998; p 143.
(30) Gonzalez-Lafont, A.; Truong, T. N.; Truhlar, D. G. *J. Phys. Chem.* **1991**, *95*, 4618.
(31) Liu, Y.-P.; Lu, D.-h.; Gonzalez-Lafont, A.; Truhlar, D. G.; Garrett, B. C. *J. Am. Chem. Soc.* **1993**, *115*, 7608.
(32) The results of the present work confirm the validity of this assumption.
(33) Steinfeld, J. I.; Francisco, J. S.; Hase, W. L. *Chemical Kinetics and Dynamics*; Prentice Hall: Englewood Cliffs, NJ, 1989.
(34) Schroeder, J.; Schwarzer, D.; Troe, J.; Voss, F. *J. Chem. Phys.* **1990**, *93*, 2393.
(35) Courtney, S. H.; Balk, M. W.; Philips, L. A.; Webb, S. P.; Yang, D.; Levy, D. H.; Fleming, G. R. *J. Chem. Phys.* **1988**, *89*, 6697.
(36) Field, M. J.; Bash, P. A.; Karplus, M. *J. Comput. Chem.* **1990**, *11*, 700.

(37) Carmer, C. S.; Weiner, B.; Frenklach, M. *J. Chem. Phys.* **1993**, *99*, 1356.
(38) Eichler, U.; Kölmel, C. M.; Sauer, J. *J. Comput. Chem.* **1996**, *18*, 463.
(39) Tuñón, I.; Martins-Costa, M. T. C.; Millot, C.; Ruiz-López, M. F. *J. Chem. Phys.* **1997**, *106*, 3633.
(40) Baer, T.; Hase, W. L. *Unimolecular Reaction Dynamics: Theory and Experiments*; Oxford University Press: New York, 1996.
(41) Dewar, M. J. S.; Hashmall, J. A.; Venier, C. G. *J. Am. Chem. Soc.* **1968**, *90*, 1953; Dewar, M. J. S.; Trinajstic, N. *J. Chem. Soc. (A)* **1971**, 1220.
(42) Stewart, J. P. P. MOPAC 7.0, a General Molecular Orbital Package. *QCPE* **1993**, 455. Stewart, J. P. P. *J. Comput. Chem.* **1989**, *10*, 209.
(43) Dewar, M. J. S.; Zoebisch, E. G.; Healy, E. F.; Stewart, J. J. P. *J. Am. Chem. Soc.* **1985**, *107*, 3902.
(44) Dubnikova, F.; Lifshitz, A. *J. Phys. Chem. A* **1998**, *102*, 3299.
(45) Lim, K. F.; Gilbert, R. G. *J. Phys. Chem.* **1990**, *94*, 77.
(46) Allen, M. P.; Tildesley, D. J. *Computer Simulation of Liquids*; Clarendon Press: Oxford, 1996.
(47) Nyman, G.; Nordholm, S.; Schranz, H. W. *J. Chem. Phys.* **1990**, *93*, 6767.
(48) Chapman, S.; Bunker, D. L. *J. Chem. Phys.* **1975**, *62*, 2890; Sloane, C. S.; Hase, W. L. *J. Chem. Phys.* **1977**, *66*, 1523.
(49) Hase, W. L. *J. Chem. Phys.* **1976**, *64*, 2442.
(50) Truhlar, D. G.; Garrett, B. C. *Acc. Chem. Res.* **1980**, *13*, 440.
(51) Truhlar, D. G.; Hase, W. L.; Hynes, J. T. *J. Phys. Chem.* **1983**, *87*, 2664.
(52) Robinson, P. J.; Holbrook, K. A. *Unimolecular Reactions*; Wiley-Interscience: New York, 1972.
(53) Forst, W. *Theory of Unimolecular Reactions*; Academic Press: New York, 1973.
(54) Wilson, E. B., Jr.; Decius, J. C.; Cross, P. C. *Molecular Vibrations*; McGraw-Hill: New York, 1955.
(55) Bunker, D. L. *Meth. Comput. Phys.* **1971**, *10*, 287.
(56) Press, W. H.; Teukolsky, S. A.; Vetterling, W. T.; Flannery, B. P. *Numerical Recipes in Fortran*; *The art of scientific computing*; University Press: Cambridge, 1992.
(57) Peslherbe, G. H.; Hase, W. L. VENUS-MOPAC, a General Chemical Dynamics and Semiempirical Direct Dynamics Computer Program. To be released.
(58) Berendsen, H. J. C.; Postma, J. P. M.; van Gunsteren, W. F.; DiNola, A.; Haak, J. R. *J. Chem. Phys.* **1984**, *81*, 3684.
(59) Nosé, S. *Mol. Phys.* **1984**, *52*, 255; Hoover, W. G. *Phys. Rev. A* **1985**, *31*, 1695.
(60) Hansen, J.-P.; McDonald, I. R. *Theory of Simple Liquids*; Academic Press: London, 1990.
(61) At these high densities the steric effect of the Ar bath may best be visualized as a cage effect where the Ar atoms do not have large amplitude motion on the time scale of the trimethylene decomposition. The Ar bath can thus be considered as a static environment which forms a cage around the decomposing trimethylene.
(62) Nikowa, L.; Schwarzer, D.; Troe, J.; Schroeder, J. *J. Chem. Phys.* **1992**, *97*, 4827.
(63) Peslherbe, G. H.; Hase, W. L. *J. Chem. Phys.* **1996**, *104*, 7882.
(64) Peslherbe, G. H.; Wang, H.; Hase, W. L. *J. Am. Chem. Soc.* **1996**, *118*, 2257.
(65) Schinke, R.; Engel, V. *Faraday Discuss. Chem. Soc.* **1986**, *82*, 111. Schinke, R. *J. Chem. Phys.* **1990**, *92*, 2397; Schinke, R. *Photodissociation dynamics*; Cambridge: New York, 1993.
(66) Wyatt, R. E.; Iung, C.; Leforestier, C. *J. Chem. Phys.* **1992**, *97*, 3477.
(67) Untch, A.; Schinke, R.; Cotting, R.; Huber, J. R. *J. Chem. Phys.* **1993**, *99*, 9553.
(68) Chen, W.; Hase, W. L.; Schlegel, H. B. *Chem. Phys. Lett.* **1994**, *228*, 436.
(69) Dobbyn, A. J.; Stumpf, M.; Keller, H.-M.; Schinke, R. *J. Chem. Phys.* **1996**, *104*, 8357.
(70) *Advances in Classical Trajectory Methods*: *Comparison of Classical and Quantum Dynamics*; Hase, W. L., Ed.; JAI Press: London, 1998; Vol. 3.
(71) Goldfield, E. M. *J. Chem. Soc. Faraday Disc.* **1998**, *110*, 185.
(72) Hase, W. L.; Buckowski, D. G. *J. Comput. Chem.* **1983**, *3*, 335.
(73) Lu, D. H.; Hase, W. L. *J. Chem. Phys.* **1988**, *89*, 6723.
(74) Peslherbe, G. H.; Hase, W. L. *J. Chem. Phys.* **1996**, *104*, 9445.
(75) The possible effect of "zpe pooling", from high-frequency CH stretch and bending modes of trimethylene, was indirectly tested in this work by comparing results for two sampling schemes which put different initial amounts of energy into these modes (see Tables 1 and 2).
(76) Hase, W. L.; Darling, C. L.; Zhu, L. *J. Chem. Phys.* **1992**, *96*, 8295.
(77) Fredj, E.; Gerber, R. B.; Ratner, M. A. *J. Chem. Phys.* **1998**, *109*, 4833.
(78) Wang, J.-C.; Fichthorn, K. A. *J. Chem. Phys.* **1998**, *109*, 10138.
(79) Martyna, G. J.; Tuckerman, M. E.; Tobias, D. J.; Klein, M. L. *Molecular Physics* **1996**, *87*, 1117; Tuckerman, M. E.; Berne, B. J.; Martyna, G. J. *J. Chem. Phys.* **1992**, *97*, 1990 (and the references within).
(80) Watanabe, M.; Karplus, M. *J. Chem. Phys.* **1993**, *99*, 8063.
(81) Verlet, L. *Phys. Rev.* **1967**, *159*, 98.
(82) Ishida, H.; Naga, Y.; Kidera, A. *Chem. Phys. Lett.* **1998**, *282*, 115.
(83) Gray, S. K.; Noid, D. W.; Sumpter, B. G. *J. Chem. Phys.* **1994**, *101*, 4062.
(84) Martyna, G. J.; Tuckerman, M. E. *J. Chem. Phys.* **1995**, *102*, 8071.